Published for SISSA by Springer

Received: *December 7, 2023*
Revised: *April 21, 2024*
Accepted: *May 2, 2024*
Published: *May 24, 2024*

A neutrino floor for the Migdal effect

Gonzalo Herrera

Center for Neutrino Physics, Department of Physics, Virginia Tech, Blacksburg, VA 24061, U.S.A.
Physik-Department, Technische Universität München, James-Franck-Straße, 85748 Garching, Germany
Max-Planck-Institut für Physik (Werner-Heisenberg-Institut), Föhringer Ring 6, 80805 München, Germany

E-mail: gonzaloherrera@vt.edu

Abstract: Neutrino-nucleus scatterings in the detector could induce electron ionization signatures due to the Migdal effect. We derive prospects for a future detection of the Migdal effect via coherent elastic solar neutrino-nucleus scatterings in liquid xenon detectors, and discuss the irreducible background that it constitutes for the Migdal effect caused by light dark matter-nucleus scatterings. Furthermore, we explore the ionization signal induced by some neutrino electromagnetic and non-standard interactions on nuclei. In certain scenarios, we find a distinct peak on the ionization spectrum of xenon around 0.1 keV, in clear contrast to the Standard Model expectation.

Keywords: Neutrino Interactions, Non-Standard Neutrino Properties, Particle Nature of Dark Matter

ArXiv ePrint: 2311.17719

https://doi.org/10.1007/JHEP05(2024)288

Contents

1 Introduction

In some problems in perturbation theory, the time of action of the perturbation can be small, while the perturbation itself does not need to be weak. One example of this circumstance is the ionization due to β decay. The velocity of the outgoing electron is much larger than the velocity of the atomic electrons, thus, from the reference frame of the atomic electrons, the change in the nuclear charge occurs suddenly. The sudden approximation in Quantum Mechanics then allows to compute transition probabilities in systems whose wavefunction is not substantially changed, $\Phi(t) \approx \Phi(0)$.

One interesting application of the sudden approximation was proposed by Migdal in 1939 [1], later discussed in his textbook in Quantum Mechanics [2]. In nuclear collisions involving large energy transfers, ionization of the recoil atoms is likely to occur. If the velocity of the nucleus is small, then it carries its electrons off with it. For large velocities, on the other hand, the nucleus recoils out of its electronic shells and electrons do not have time to catch up with the nucleus motion. Evidence for the Migdal effect has been reported in measurements of compton scattering of neutrons in hydrogen [3], and in some nuclear decay processes [4]. Further, there are some experimental proposals aiming to observe the Migdal effect from nuclear recoils of Standard Model particles in the near future [5–7]. A first dedicated search in liquid xenon from neutron scatters was already performed, albeit finding no signal consistent with the model expectations [8]. This may indicate that the theoretical uncertainties are large and difficult to quantify [9, 10].

The importance of the contribution from the Migdal effect for direct dark matter searches was initially discussed in [11–13], and several subsequent studies have followed in recent years, *E.g* [9, 10, 14–29]. The ionization signal from the Migdal effect is suppressed w.r.t. the nuclear one, but there is a range of energies where the nuclear recoil energy falls below threshold while the electromagnetic signal is observable.

Moreover, it has been pointed out for some years that direct detection experiments, originally designed to detect scatterings of dark matter particles from the Milky Way halo with the detector, could also be used to study solar neutrino physics (in the Standard Model and beyond), *E.g* [30–37]. Crucially, it has been claimed that scatterings of solar neutrinos off nuclei in the Standard Model may constitute an irreducible background for direct dark matter searches, the so-called neutrino "floor", or neutrino "fog" [38–41].

JHEP05(2024)288

In this work, we aim to study the current possibilities and future prospects to detect the Migdal effect electronic ionization induced by coherent elastic neutrino-nucleus scattering at Earth-based liquid xenon detectors, and its distinguishability from a light dark matter induced signal.

In particular, we consider in detail the full low-energy neutrino flux at Earth stemming from processes in the Sun such as the proton-electron-proton reaction (*pep*), the *hep* branch, the ^{7}Be line, the β^+ decay processes, ^{13}N, ^{15}O and ^{17}F, as well as the contribution from the diffuse supernova neutrino background and atmospheric neutrinos [42, 43]. It should be noted that previous works calculated the Migdal ionization rate induced by solar neutrinos from *pp*, ^{8}B, *pep* and ^{7}Be processes, plus the atmospheric neutrino flux [14, 17]. Most of the additional neutrino fluxes that we include in our calculation are largely subdominant with respect to these, with the exception of the ^{13}N, ^{15}O and ^{17}F processes, which dominate in certain energy regions between $\sim 420\,\text{keV}$ and $\sim 1800\,\text{keV}$, in between the *pp* and ^8B fluxes [32]. Further, we will confront our results with XENON1T (S2-only) data [44], and with the expected signal from light dark matter-electron scatterings, in order to discuss its discriminability. Additionally, we will study the ionization signal induced by solar neutrino scatterings off nuclei due to electromagnetic and non-standard interactions.

The paper is organized as follows: in section 2, we will introduce the relevant formalism and calculate the Migdal ionization rate induced by CEνNS in liquid xenon, further confronting it with the signal induced by light dark matter-nucleus scatterings, and deriving the neutrino "floor" induced by the Migdal effect. Further, we derive projections on the future detectability of the Migdal effect induced by solar neutrino-nucleus scatterings in XENONnT. In section 3, we will calculate the ionization rate induced by electromagnetic and some non-standard neutrino-nucleus interactions, noticing a distinct feature on the ionization spectrum around 0.1 keV in some beyond the Standard Model scenarios arising from the ionization of electrons in the $n = 4$ shell by *pp*-chain solar neutrinos. Finally, in section 4, we will present our conclusions.

2 Migdal ionization rate due to CEνNS and dark matter-nucleus scatterings

The CEνNS process can induce ionization through the Migdal effect. The differential cross-section for this process is [2, 14, 17, 45]

$$\frac{d\sigma_{\nu N-\nu N^* e^-}}{dE_R} = \frac{G_F^2 m_A}{4\pi} Q_V^2 \left(1 - \frac{m_A E_R}{2E_\nu^2}\right) \times |Z_{ion}(E_{er})|^2 \tag{2.1}$$

where m_A is the target mass. Q_V is the vector charge of the nucleus and reads

$$Q_V = g_{pV} Z F_p\left(E_R\right) + g_{nV} N F_n\left(E_R\right) \tag{2.2}$$

and F_p and F_n are the proton and neutron form factor, respectively, for which we adopt the Helm prescription with proton and neutron root mean square radius of and $R_p = 3.14\,\text{fm}$ and $R_n = 3.36\,\text{fm}$. Z and N are the number of protons and neutrons in the nucleus, and the neutral current vector couplings, g_{pV} and g_{nV} are

$$g_{pV} = \frac{1}{2} - 2\sin^2\theta_W \tag{2.3}$$

JHEP05(2024)288

$$g_{nV} = -\frac{1}{2} \tag{2.4}$$

where the weak mixing angle is taken as $\sin^2\theta_W \simeq 0.237$. The ionization form factor $|Z_{ion}(E_{er})|^2$ is given by

$$|Z_{ion}(E_{er})|^2 = \frac{1}{2\pi}\sum_{n,l}\int dE_{er}\frac{d}{dE_{er}}p(nl \to E_{er}) \tag{2.5}$$

where the ionization probability of an electron in the orbital (n, l) is denoted by p. We take the tabulated values of the ionization probabilities for xenon from [14], accounting for the orbitals $5p$, $5s$, $4d$, $4p$, $4s$, $3d$, $3p$ and $3s$. E_{er} refers to the electron recoiling energy. The total ionization rate due to the Migdal effect can then be calculated as

$$\frac{dR^{\rm mig}}{dE_R} = N_T\int_{E_v^{\rm min}}^{E_v^{\rm max}}\frac{d\Phi}{dE_v}\frac{d\sigma_{\nu N\to\nu N^* e^-}}{dE_R}dE_v \tag{2.6}$$

where $\frac{d\Phi}{dE_v}$ is the differential neutrino flux. We take all known solar, atmospheric and diffuse supernova background contributions from [42]. N_T is the number of target nuclei in the detector. Finally, the detector energy $E_{\rm det}$ measured at liquid xenon experiments like XENONnT is obtained by convolving the integration of the nuclear recoil rates with $\delta(E_{\rm det} - q_{nr}E_R - E_{er} - E^{nl})$, where E_R is the nuclear recoil energy, E_{er} is the ionized electron recoiling energy, E^{nl} is the orbital binding energy and q_{nr} is the conversion factor from nuclear to electron equivalent energy. We take $q_{nr} = 0.15$ [46]. The limits of integration over nuclear recoil energies are given by

$$E_R^{\rm min} = \frac{\left(E_{er} + E^{nl}\right)^2}{2m_A} \tag{2.7}$$

$$E_R^{\rm max} = \frac{\left(2E_\nu - \left(E_{er} + E^{nl}\right)\right)^2}{2\left(m_A + 2E_\nu\right)}. \tag{2.8}$$

Dark matter particles can also induce ionization via Migdal effect in nuclear scatterings. The rate of ionization events due to the Migdal effect corresponds to the standard dark matter-nucleus differential recoil rate multiplied by the ionization rate

$$\frac{d^2R^{\rm mig}}{dE_R dv} = \frac{d^2R}{dE_R dv}\times|Z_{ion}(E_{er})|^2 \tag{2.9}$$

where, for a given nucleus i

$$\frac{d^2R}{dE_R dv} = \mathcal{F}(\vec{v})\frac{{\rm d}\sigma_i}{{\rm d}E_R}(v, E_R) \tag{2.10}$$

where $\mathcal{F}(\vec{v})$ is the total dark matter flux reaching the Earth. We assume the so called Standard Halo Model (SHM), with a local dark matter density of $\rho_{\rm DM} = 0.3\,{\rm GeV/cm^3}$ and a Maxwellian velocity distribution truncated at the escape velocity of the Milky Way, such that

$$\mathcal{F}(\vec{v}) = \frac{\rho_{\rm DM}}{m_{\rm DM}}v f_{\rm MB}(\vec{v}) \tag{2.11}$$

JHEP05(2024)288

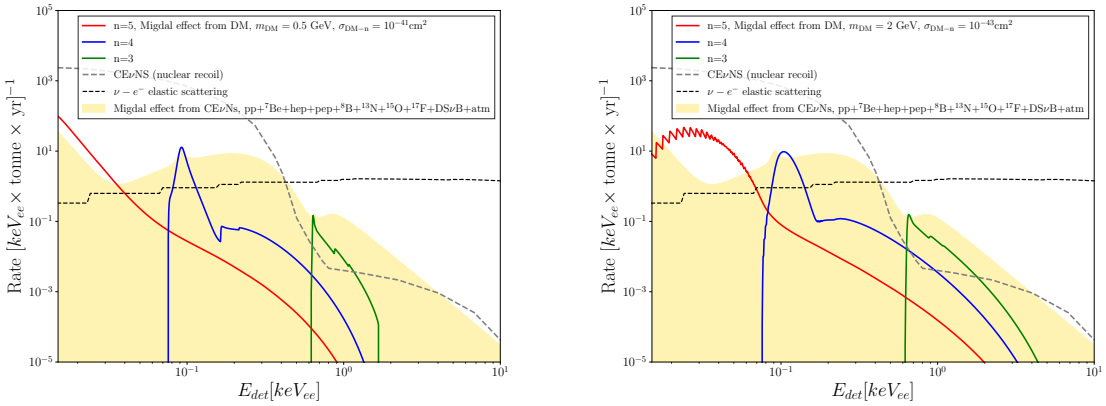

Figure 1. *Left plot*: comparison of the Migdal ionization rate induced by CEνNS in xenon (yellow) and the Migdal ionization rate induced by a light dark matter particle with mass of $m_{\rm DM} = 0.5\,{\rm GeV}$ and cross section with nucleons $\sigma_{\rm DM-n} = 10^{-41}$ cm^2, where we separate the contribution from the shells $n = 5$ (red), $n = 4$ (blue) and $n = 3$ (green). For comparison, we show the nuclear recoil signal from CEνNS (grey), and the electron ionization signal from elastic neutrino-electron scatterings (black). *Right plot*: similar plot, for a heavier dark matter particle of mass $m_{\rm DM} = 2\,{\rm GeV}$ and $\sigma_{\rm DM-n} = 10^{-43}$ cm^2.

where the Maxwell-Boltzmann velocity distribution in the galactic frame is defined as

$$f_{\rm MB}(\vec{v}) = \frac{1}{(2\pi\sigma_v^2)^{3/2}\,N_{\rm esc}} \exp\left[-\frac{v^2}{2\sigma_v^2}\right] \qquad \text{for } v \leq v_{\rm esc}, \tag{2.12}$$

and here, $v = |\vec{v}|, \sigma_v = 156$ km/s is the velocity dispersion [47], and $v_{\rm esc} = 544$ km/s is the escape velocity from our galaxy [48]. $N_{\rm esc}$ is a normalization constant with value $N_{\rm esc} \simeq 0.993$. We point out that further contributions to the total dark matter flux on Earth and corrections to the SHM are expected, *E.g* [49–53], but an analysis on the impact of these on the Migdal ionization rate is beyond the scope of our work, and left for future studies.

For the differential dark matter-nucleus scattering cross section, we assume for simplicity an isoscalar spin-independent dark matter-nucleus interaction, with equal couplings of dark matter to all nucleons

$$\frac{d\sigma_i^{\rm SI}}{dE_R}(v, E_R) = \frac{m_{A_i}}{2\mu_{\rm DM-n}^2 v^2} A_i^2 \sigma_{\rm DM-n} F_i^2\,(E_R) \tag{2.13}$$

where $\sigma_{\rm DM-n}$ is the non-relativistic dark matter-nucleon scattering cross section

With this, after integrating equation (2.6) over the velocity distribution of the dark matter particles, we can calculate the ionization rate as a function of the detector energy. We implement our own code for all these tasks, finding good agreement with previous literature on the topic, *E.g* [14]. In figure 1 we show the rate of events in xenon in tonnes × year from the Migdal ionization rate from CEνNs, including the full neutrino flux at Earth at MeV energies. We compare this with the nuclear recoil signal from CEνNs, and the electron ionization signal from neutrino-electron scattering. The Migdal ionization signal is expected to dominate over the neutrino-electron scattering signal below $\sim 0.4\,{\rm keV}_{ee}$, and over the nuclear recoil signal from $\sim 0.4 - 4\,{\rm keV}_{ee}$. Further, we show the signal rate induced by the Migdal effect

JHEP05(2024)288

from nuclear scatterings of sub-GeV dark matter particles, including the contributions from the outer shells, for different values of the dark matter mass and scattering cross section with nucleons. As apparent in the plot, for such values, the irreducible background from solar neutrinos would mask the signal induced by light dark matter inducing ionizations via nuclear scatterings and the Migdal effect. This indicates that the neutrino floor for the Migdal effect induced by light dark matter-nucleon scatterings in xenon-based detectors can be present already for cross sections of $\sigma_{\mathrm{DM-p}} \sim 10^{-42}$ cm^2. Current upper limits on the Migdal effect from light dark matter-nucleon scattering constrain values of $\sigma_{\mathrm{DM-p}} \sim 10^{-38}$ cm^2 at $m_{\mathrm{DM}} \sim 0.5\,\mathrm{GeV}$ [44], so there is yet roughly 4 orders of magnitude in sensitivity to explore before needing to fit accurately the neutrino floor for the Migdal effect, in order to claim a potential detection of light dark matter particles in the future.

This qualitative discussion from figure 1 can be extended more quantitatively by deriving the neutrino floor for the Migdal effect signal from dark matter, in the parameter space of dark matter mass vs scattering cross section. As a criteria to find the values of the dark matter-nucleon scattering cross section corresponding to the neutrino floor, we impose that the ionization rate from CEνNs should exceed the ionization rate induced by dark matter over the relevant electron recoil energy range of xenon-based experiments. Under this criteria, the dark matter signal would be "masked" by the neutrino signal, however, we remind that with sufficient statistics and via spectral analyses, both contributions might be distinguishable. Indeed, it has been long discussed that the neutrino floor should be rather regarded as the neutrino "fog".

In the left plot of figure 2 we derive the neutrino floor induced by the Migdal ionization signal from CEνNS in Xenon, and confront it with upper limits derived from the Migdal effect in XENON1T (S2 only and S1-S2 analyses), LUX, CDEX and the EDELWEISS experiments. As can be appreciated in the figure, for dark matter masses between $m_{\mathrm{DM}} \sim 0.5 - 2\,\mathrm{GeV}$, current sensitivity of XENON1T allows to explore less than four orders of magnitude in the values of the dark matter-nucleon scattering cross section, before the neutrino floor is reached. For dark matter masses between $m_{\mathrm{DM}} \sim 0.08 - 0.5\,\mathrm{GeV}$, this range extends from 4 to 5 orders of magnitude, and for even lower dark matter masses, the neutrino floor is as far as 7 orders of magnitude from current sensitivity.

Given the substantial increase in sensitivity at XENONnT, LUX-ZEPLIN and PANDA-X most recent runs [57–59], it is plausible to speculate that dedicated analysis on the Migdal effect with near future data may allow to detect the ionization contribution from the Migdal effect due to CEνNS. In the following, we calculate the projected impact of ionizations due to Migdal effect in the XENONnT experiment.

The lowest electron recoiling energies reached by XENON are found in the S2-only data analysis [44], with energy threshold as small as $0.2\,\mathrm{keV}_{ee}$. At slightly lower energies, the observed rate is significantly larger than the background prediction, but the collaboration claims no excess due to lack of knowledge on the background at such low energies, and due to their small efficiency. In the following, we study directly the detectability of the Migdal effect from CEνNS for current exposures from XENONnT experiment [60], and assuming a similar background and signal per tonne $\times$ year as XENONnT analysis [57], and same efficiency function as in XENON S2-only analysis [44]. The most recent XENONnT analysis of electron recoil data achieved an astonishing low background level in the 1–30 keV region of 15.8 ± 1.3 events per tonne $\times$ year $\times$ keV. We will consider this background level for our projection,

JHEP05(2024)288

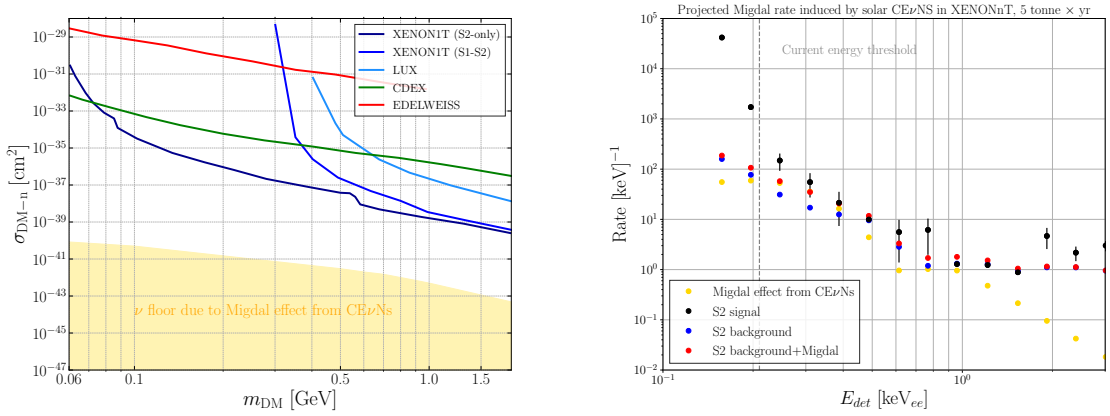

Figure 2. *Left plot*: neutrino floor in Xenon due to the ionization of electrons following the coherent elastic neutrino-nucleus scattering. For comparison, we show current upper limits on the light dark matter-nucleon scattering cross section from the Migdal effect in XENON1T [46], LUX [54], CDEX [55], and EDELWEISS [56]. *Right plot*: projected rate of Migdal ionization events in XENONnT from the CEνNs, and its distinguisability from the background events. See main text for further details.

assuming it might be preserved at the lower recoil energies considered in previous S2-only data analysis. Furthermore, we neglect the neutrino-electron scattering signal in our analysis, which is expected to dominate over the Migdal induced signal at energies above 1 keV, but is subdominant by 1 to 2 orders of magnitude in the energy range from $\sim 0.01 to \sim 0.4$ keV, where the Migdal signal from neutrinos might be detected.

In the right panel of figure 2, we show our results. The Migdal effect induced by CEνNs is expected to dominate over current low-energy backgrounds for a XENON1T S2-like data in the energy range from 0.1 to 1 keV$_{ee}$ for exposures of $\sim$ tonnes $\times$ year, and background levels between 1 to 10 events per $\sim$keV $\times$ year $\times$ tonne, as was recently achieved in the energy range from 1 to 10 keV in XENONnT [60]. Thus, the contribution from the Migdal effect is expected to become sizable in the future. At larger energies than 1 keV$_{ee}$, the sensitivity reach would need to be improved by orders of magnitude. Lowering threshold and background levels at low-energies will be crucial for the detection of the Migdal effect from neutrinos. This, in turn, is a necessary task to be able to detect the Migdal effect induced by light dark matter scatterings off nuclei in the detector. It should be noted, however, that in our analysis we are assuming a future data set analogous to the most recent XENON1T S2-only data, but in reality we are assuming that the nuclear recoil can be told apart from the electron recoil signal, either via a combined S1-S2 analysis, or via a dedicated spectral analysis, that could differentiate the nuclear from the Migdal ionization signals. Also, the current energy threshold of the XENON1T collaboration for the combined S1-S2 data is not as small as that in the XENON1T S2-only analysis, so our projections will only apply if the energy threshold for a combined S1-S2 analysis is reduced in the future.

3 The ionization signal induced by electromagnetic and non-standard neutrino-nucleus scatterings

Neutrinos are neutral particles in the Standard Model, but are guaranteed to interact electromagnetically at one-loop with nuclei via multipoles. The number of this multipoles

JHEP05(2024)288

allowed and whether they are diagonal or off-diagonal depends on the Majorana or Dirac nature of the neutrino [61–63].

If neutrinos scatter coherently on nuclei via a magnetic moment, the associated ionization due to the Migdal effect has cross section [64]

$$\left(\frac{\mathrm{d}\sigma_{\nu N\to\nu N^* e^-}}{\mathrm{d}E_R}\right)_\mu = \frac{\pi\alpha^2\mu^2_{\nu,\mathrm{eff}}Z^2}{m_e^2}\left(\frac{1}{E_R}-\frac{1}{E_\nu}+\frac{E_R}{4E_\nu^2}\right)F_p^2\left(E_R\right)\times\left|Z_{ion}(E_{er})\right|^2 \tag{3.1}$$

where $\mu_{\nu,\mathrm{eff}}$ is the effective magnetic moment of solar neutrinos, which comprises a sum of the contributions of each mass eigenstate weighted by the entries of the PMNS matrix [63]

$$\mu^2_{\nu,\mathrm{eff}} = \sum_k |U_{ek}|^2 \sum_j |\mu_{jk} - ie_{jk}|^2 \tag{3.2}$$

where U is the PMNS matrix (which should account for matter effects in the Sun), μ_{jk} are the magnetic multipoles of the mass eigenstates, and e_{jk} are the electric dipole moments of the mass eigenstates, which is degenerate with the magnetic moment for our recoil rate observable.

Neutrinos are expected to scatter off nuclei also via their anapole moment. In fact, this is the only diagonal moment allowed for Majorana neutrinos. This contribution interferes with the weak current, and the interference can be parametrized via a redefinition of the weak mixing angle in equation (2.1)

$$\sin^2\theta_W \to \sin^2\theta_W\left(1-2m_W^2 a_{\nu,\mathrm{eff}}\right) \tag{3.3}$$

where the effective anapole moment is defined similarly as the magnetic moment via

$$a_{\nu,\mathrm{eff}} = \sum_k |U_{ek}| \sum_j a_{jk} \tag{3.4}$$

In figure 3, we show the electron ionization rate from neutrino-nucleus scattering due to the weak current compared to the magnetic moment contribution and the anapole moment contribution. We show the ionization rates for values which yield rates comparable or larger than the expected contribution from CEνNS. From this figure it becomes evident that values of the effective magnetic moment as low as $\sim 5\times10^{-13}\mu_B$ and values of the effective anapole moment as low as $\sim 10^{-32}\mathrm{cm}^2$ could be probed via the Migdal effect in future XENONnT analysis. This value of the magnetic moment might be stronger than current laboratory constraints [60, 65], and the value of the anapole moment is close to the Standard Model values [66]. As expected, the spectral shape of the anapole moment induced ionization rate is the same as the ionization caused by CEνNS, while the magnetic moment induced ionization rate differs from the Standard Model, due to a dominance of the signal from pp-neutrinos w.r.t. the signal from the more energetic neutrino fluxes. This is caused by an enhancement on the neutrino-nucleus scattering cross section via a magnetic moment at low incoming neutrino energies.

The electromagnetic scattering of neutrinos off nuclei is expected to occur in the Standard Model. However, neutrinos may also interact beyond the Standard Model. A simple example consists in neutrinos coupling to quarks via new light scalar or vector mediators. The coherent scattering off nucleus would then also cause an ionization signal due to the Migdal effect. For

JHEP05(2024)288

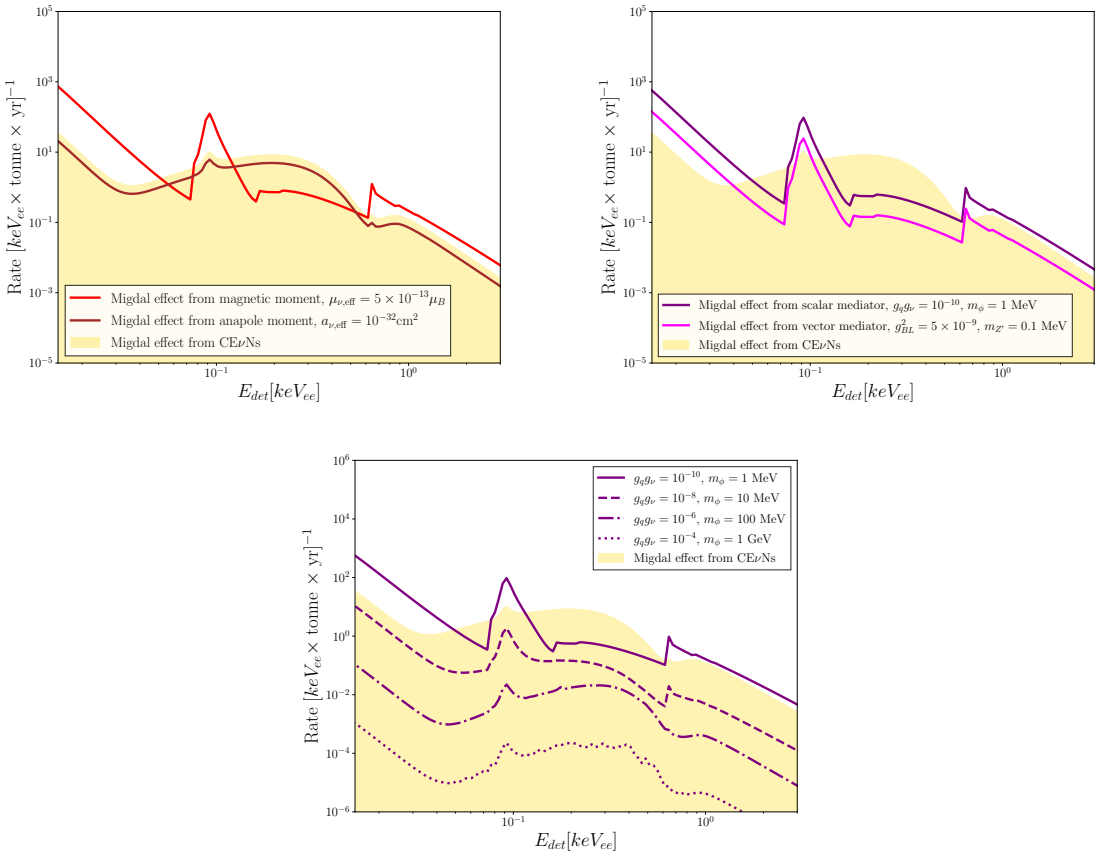

Figure 3. *Upper left plot*: ionization spectrum of xenon from the Migdal effect due to CEνNS in the Standard Model (yellow), due to an anapole moment interaction (brown) and due to a magnetic moment interaction (red). For comparison, we show the measured data and background expectation from XENON1T S2-only analysis [44]. *Upper right plot*: similar plot, but this time confronting the Standard Model expectation with the signal induced by neutrino-nucleus interactions mediated by a new scalar particle (purple) or by a new $B-L$ vector mediator (magenta). *Lower plot:* ionization spectrum induced by a scalar mediator, for different values of its mass. We illustrate how the peak around 0.1 keV$_{ee}$ is smoothed out for sufficiently heavy mediators, due to the dominance of the more energetic part of the neutrino flux over *pp* neutrinos.

a scalar mediator there is no interference with the Standard Model contribution, and the Migdal ionization signal from neutrino-nucleus scattering reads [67–69]:

$$\left(\frac{d\sigma_{\nu N-\nu N^* e^-}}{dE_R}\right)_\phi = \frac{G_F^2 m_A^2}{4\pi} \frac{g_{\nu\phi} Q_\phi^2 E_R}{E_\nu^2 \left(2m_A E_R + m_\phi^2\right)^2} \times |Z_{ion}(E_{er})|^2 \tag{3.5}$$

where the scalar charge is defined as [70]

$$Q_\phi = Z F_p(E_R) \sum_{q=u,d} g_{q\phi} \frac{m_p}{m_q} f^p_{T_q} + N F_n(E_R) \sum_{q=u,d} g_{q\phi} \frac{m_n}{m_q} f^n_{T_q} \tag{3.6}$$

and we take values of the hadronic form factors $f^p_{T_q}$ and $f^n_{T_q}$ from [71]. Further, we will assume for simplicity that the scalar ϕ couples to quarks u and d with same strength, $g_{u\phi} = g_{d\phi}$.

JHEP05(2024)288

For the vector mediator case, there is interference with the weak scattering contribution. The interference can be parametrized through a redefinition of the weak vector charge in equation (2.1) [72]:

$$Q_V \to Q_{Z'} = Q_V + \frac{g_{\nu Z'}}{\sqrt{2}G_F} \frac{(2g_{uZ'}+g_{dZ'})\,ZF_p(E_R)+(g_{uZ'}+2g_{dZ'})\,NF_n(E_R)}{2m_A E_R+m_{Z'}^2} \tag{3.7}$$

where again we assume universal quark couplings to the vector mediator, $g_{uZ'} = g_{dZ'}$. We will focus in a concrete $\mathrm{U}(1)_{B-L}$ extension of the Standard Model where the difference of baryon and lepton numbers is gauged. In this case, the coupling of the Z' to neutrinos and quarks is related via $g_{qZ'} = -g_{\nu Z'}/3$ [72–74].

In figure 3, we show the ionization rates induced via the Migdal effect in these models, for values of the couplings and mediator masses currently allowed in parameter space by other experiments. For mediator masses around 1 MeV, strong constraints on couplings of order $g^2 \lesssim 10^{-9} - 10^{-10}$ arise from CEνNs of reactor neutrinos in nearby detectors [69, 75], from solar neutrino-electron scattering in Borexino [76–79], and from solar neutrino-nucleus scatterings in direct detection experiments [80–84]. It can be appreciated in the figure that for the vector mediator model from a $\mathrm{U}(1)_{B-L}$ symmetry, the ionization rate falls below the expected rate in the Standard Model, so a detection of the Migdal effect from CEνNS with some precision would be needed to set strong constraints in this model. However, for the scalar mediator case, and for currently allowed values of the mediator mass and couplings, the expected scattering rate can be higher than in the Standard Model, which clearly suggests that ionization signals in liquid xenon detectors may be a good probe of these models in the near future. It should be noted, however, that if discrimination of nuclear and electron recoil events at low energies becomes possible, the nuclear recoil signal is expected to provide stronger limits than the Migdal signal, due to the larger total rate. However, the Migdal signal yields a rate with a more peculiar spectral form, which may enhance discrimination from other backgrounds.

As we already mentioned, the spectral shape of the ionization rate due to a neutrino magnetic moment or due to new light mediators differs from the one induced by the weak interactions. This is due to the fact that solar *pp* neutrinos, with lower energies, contribute predominantly to the ionization signal due to the enhancement in the cross section at low energies in these models. For the Standard Model contribution to the scattering rate, on the other hand, the larger energy neutrino flux from other processes in the Sun, and from the atmospheric and diffuse supernova neutrino background contributes predominantly. The Migdal effect then provides a remarkable feature of new physics in the neutrino sector, which is a peak in the ionization spectrum around 0.1 keV given by the ionization of the electrons in the $n = 4$ shell from solar *pp* neutrinos. This spectral feature differs largely from the scattering rate due to CEνNS in the Standard Model.

In the lower plot of the figure we show the ionization rate induced in the scalar mediator model, for different values of the scalar mediator mass. As the mediator mass becomes larger, the contributions to the scattering rate from the neutrino flux on Earth above ~ 400 keV energies becomes dominant with respect to the *pp* neutrinos, and the peak in the spectrum around ~ 0.1 keV electron energies is smoothed out substantially.

JHEP05(2024)288

We believe that near future liquid xenon experiments should be able to resolve such a peak on the spectrum after accounting for energy resolution effects, experimental efficiencies, and background modellings. On the one hand, the main background at such energies in XENON1T is given by events from β decays on the cathode wires, which seem to increase linearly at low energies. There is no reason to think that they should peak at $0.1\,\mathrm{keV}_{ee}$ with small width. Further, the energy resolution of electron recoil events in XENON1T is smaller than the predicted width of the peak we are discussing, which goes from $0.06\,\mathrm{keV}_{ee}$ to $0.12\,\mathrm{keV}_{ee}$. The main drawback at this point is the minimal energy threshold and efficiency of these experiments, which currently lies at $\sim 0.2-1\,\mathrm{keV}_{ee}$ for XENON1T and LUX-ZEPLIN [44, 58]. This energy threshold would need to be reduced by roughly one order of magnitude, while keeping acceptable efficiency levels around 0.1 keV energies. We do not speculate about whether this possibility is feasible in liquid xenon detectors, but we point out that such low-energy thresholds have been achieved in recent years for bolometric detectors [85].

Of course, the peak may not manifest completely if the cross section of the new physics model is sufficiently small. Still, yet another contribution to the small peak expected in the Standard Model might be detectable even in this case. A possibility would be to confront the measured spectrum at $0.1\,\mathrm{keV}_{ee}$ with the measured spectrum around $1\,\mathrm{keV}_{ee}$, where the ionization of electrons in the $n = 3$ shell due to new physics may also differ significantly from the Standard Model, as it can be appreciated in our figures. On the other hand, if a peak is eventually detected, it might be difficult to distinguish whether it arises from neutrino-nucleus scattering or from light dark matter-nucleus scattering. As can be appreciated in figure 4, dark matter masses below $m_{\mathrm{DM}} \lesssim 0.5\,\mathrm{GeV}$ induce a peak at $0.1\,\mathrm{keV}_{ee}$ which resembles that induced by a neutrino magnetic moment, for example. If the dark matter mass is heavier, on the other hand, the width and position of the peak can vary significantly. Thus, the resolution of this spectral feature can also be used to constrain the value of the dark matter mass.

4 Conclusions

The ionization of electrons due to nuclear recoils is a quantum effect predicted in 1939, however, its observation is limited to a few anecdotal phenomena in some nuclear processes. The dubbed "Migdal effect" is expected to cause ionization of electrons on Earth based detectors sensitive to solar neutrinos via their coherent elastic scatterings off nuclei.

In this paper, we have discussed the current sensitivity and prospects for liquid xenon experiments to the ionization signal induced by coherent elastic neutrino-nucleus scattering, further quantifying the irreducible background that it constitutes for light dark matter searches based on the Migdal effect. For dark matter masses in the range from $m_{\mathrm{DM}} \sim 0.1 - 2\,\mathrm{GeV}$, we find that the neutrino floor is lying from 5 orders of magnitude to less than 4 orders of magnitude below the upper limits derived for the Migdal effect from dark matter by XENON1T.

With current exposures at XENONnT, thresholds as low as those in S2-only data, and assuming background levels as small as in their most recent analysis of electron recoil data, we find that the contribution from the Migdal effect would yield $O(1)$ changes on the detected ionization spectrum from $10^{-1}\,\mathrm{keV}_{ee}$ to $5\times10^{-1}\,\mathrm{keV}_{ee}$, with expected ionization levels due to the Migdal effect that are very close to the background level expectation.

JHEP05(2024)288

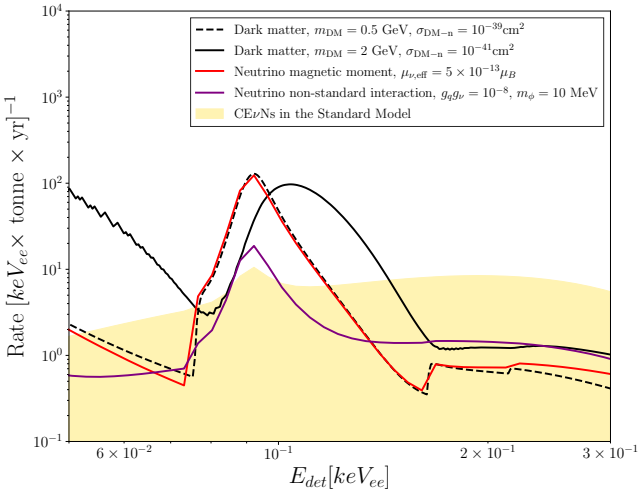

Figure 4. Zoomed ionization spectrum of xenon due to the Migdal effect from CEνNS around $0.1\,\text{keV}_{ee}$. As apparent in the plot, the ionization spectrum in the Standard Model is roughly constant around $0.1\,\text{keV}_{ee}$, with a very small peak arising from ionization of electrons in the $n = 4$ shell by *pp* solar neutrinos. However, if neutrinos interact via a magnetic moment interaction, or via new light mediators, the peak can be significantly enhanced w.r.t. to the Standard Model. Similarly, for dark matter-nucleus scattering, the Migdal effect induces a peak at those energies, although its width and central value are sensitive to the value of the dark matter mass.

We have also studied the ionization signal induced by neutrino-nucleus scatterings via an effective magnetic and anapole moments, and via new scalar or vector mediators. We find that the anapole moment may exceed the Standard Model contribution to the Migdal ionization rate for values of $a_{\nu,\text{eff}} \sim 3 \times 10^{-32}$ cm^2, and the magnetic moment contribution may be dominant for values of $\mu_{\nu,\text{eff}} \sim 5 \times 10^{-13}\mu_\text{B}$. For a scalar mediator of mass $m_\phi \sim 1 - 10\,\text{MeV}$, couplings currently allowed by complementary probes, of $g_q g_\nu \sim 10^{-11}$, would yield an ionization signal exceeding that in the Standard Model. For a $B - L$ gauged vector mediator, couplings of $g_{BL}^2 \sim 10^{-8}$ would be needed to overcome the Standard Model expectation.

For the magnetic moment interaction and new mediators with masses below $\sim 10\,\text{MeV}$, we find a distinct peak in the ionization spectrum of xenon around $0.1\,\text{keV}_{ee}$. This peak arises from the ionizations of electrons in the $n = 4$ shell due to solar neutrinos from the *pp*-chain. This peak is substantially depleted in the Standard Model, since the ionization spectrum at these energies is dominated by neutrinos with larger energies than those produced in the *pp*-chain. For these more energetic neutrinos, the ionization spectrum is continuous at $\sim 0.1\,\text{keV}_{ee}$, and the peak is almost completely smoothed out.

The ionization signal induced by the Migdal effect from CEνNS might be observed in the near future by large exposure dark matter direct detection experiments with low thresholds, becoming an irreducible background for light dark matter searches. Perhaps more importantly, this ionization signal offers a unique way to probe some models of new physics in the neutrino or dark sector, via the appeareance of a prominent peak in the ionization spectrum of xenon around $0.1\,\text{keV}_{ee}$ that is not expected to be present in the Standard Model. We hope that future data from the XENONnT, LUX-ZEPLIN and PANDA-X experiments will allow to identify the Migdal ionization signal from neutrino-nucleus scatterings, shedding light on the spectrum around $0.1\,\text{keV}_{ee}$.

JHEP05(2024)288

Acknowledgments

We are grateful to Patrick Huber for useful discussions on the Migdal effect and low-threshold direct detection experiments, and to Duncan Adams and Rouven Essig for discussions on the nuclear uncertainties present in the Migdal effect. We are also grateful to Garv Chauhan, Rijeesh Keloth, Mar Císcar and Camillo Mariani for useful discussions. We also thank Miguel Escudero, Alejandro Ibarra and Gaurav Tomar for useful feedback at the early stages of this project. The work of GH is supported by the U.S. Department of Energy Office of Science under award number DE-SC0020262, by the Collaborative Research Center SFB1258, and by the Deutsche Forschungsgemeinschaft (DFG, German Research Foundation) under Germany's Excellence Strategy - EXC-2094 - 390783311.

References

[1] A. Migdal, *Ionizatsiya atomov pri yadernykh reaktsiyakh*, *Sov. Phys. JETP* **9** (1939) 1163.

[2] A.B. Migdal, *Qualitative methods in quantum theory*, Benjamin-Cummings Publishing Co. (1977) [INSPIRE].

[3] E.B. Karlsson, O. Hartmann, C.A. Chatzidimitriou-Dreismann and T. Abdul-Redah, *The hydrogen anomaly in neutron Compton scattering: new experiments and a quantitative theoretical explanation*, *Meas. Sci. Technol.* **27** (2016) 085501.

[4] C. Couratin et al., *First measurement of pure electron shakeoff in the β decay of trapped $^6He^+$ ions*, *Phys. Rev. Lett.* **108** (2012) 243201.

[5] K.D. Nakamura et al., *Detection capability of the Migdal effect for argon and xenon nuclei with position-sensitive gaseous detectors*, *PTEP* **2021** (2021) 013C01 [arXiv:2009.05939] [INSPIRE].

[6] N.F. Bell et al., *Observing the Migdal effect from nuclear recoils of neutral particles with liquid xenon and argon detectors*, *Phys. Rev. D* **105** (2022) 096015 [arXiv:2112.08514] [INSPIRE].

[7] H.M. Araújo et al., *The MIGDAL experiment: Measuring a rare atomic process to aid the search for dark matter*, *Astropart. Phys.* **151** (2023) 102853 [arXiv:2207.08284] [INSPIRE].

[8] J. Xu et al., *Search for the Migdal effect in liquid xenon with keV-level nuclear recoils*, *Phys. Rev. D* **109** (2024) L051101 [arXiv:2307.12952] [INSPIRE].

[9] C.P. Liu, C.-P. Wu, H.-C. Chi and J.-W. Chen, *Model-independent determination of the Migdal effect via photoabsorption*, *Phys. Rev. D* **102** (2020) 121303 [arXiv:2007.10965] [INSPIRE].

[10] D. Baxter, Y. Kahn and G. Krnjaic, *Electron Ionization via Dark Matter-Electron Scattering and the Migdal Effect*, *Phys. Rev. D* **101** (2020) 076014 [arXiv:1908.00012] [INSPIRE].

[11] J.D. Vergados and H. Ejiri, *The role of ionization electrons in direct neutralino detection*, *Phys. Lett. B* **606** (2005) 313 [hep-ph/0401151] [INSPIRE].

[12] C.C. Moustakidis, J.D. Vergados and H. Ejiri, *Direct dark matter detection by observing electrons produced in neutralino-nucleus collisions*, *Nucl. Phys. B* **727** (2005) 406 [hep-ph/0507123] [INSPIRE].

JHEP05(2024)288

[13] R. Bernabei et al., *On electromagnetic contributions in WIMP quests*, *Int. J. Mod. Phys. A* **22** (2007) 3155 [arXiv:0706.1421] [INSPIRE].

[14] M. Ibe, W. Nakano, Y. Shoji and K. Suzuki, *Migdal Effect in Dark Matter Direct Detection Experiments*, *JHEP* **03** (2018) 194 [arXiv:1707.07258] [INSPIRE].

[15] M.J. Dolan, F. Kahlhoefer and C. McCabe, *Directly detecting sub-GeV dark matter with electrons from nuclear scattering*, *Phys. Rev. Lett.* **121** (2018) 101801 [arXiv:1711.09906] [INSPIRE].

[16] R. Essig, J. Pradler, M. Sholapurkar and T.-T. Yu, *Relation between the Migdal Effect and Dark Matter-Electron Scattering in Isolated Atoms and Semiconductors*, *Phys. Rev. Lett.* **124** (2020) 021801 [arXiv:1908.10881] [INSPIRE].

[17] N.F. Bell et al., *Migdal effect and photon bremsstrahlung in effective field theories of dark matter direct detection and coherent elastic neutrino-nucleus scattering*, *Phys. Rev. D* **101** (2020) 015012 [arXiv:1905.00046] [INSPIRE].

[18] S. Knapen, J. Kozaczuk and T. Lin, *Migdal Effect in Semiconductors*, *Phys. Rev. Lett.* **127** (2021) 081805 [arXiv:2011.09496] [INSPIRE].

[19] G. Grilli di Cortona, A. Messina and S. Piacentini, *Migdal effect and photon Bremsstrahlung: improving the sensitivity to light dark matter of liquid argon experiments*, *JHEP* **11** (2020) 034 [arXiv:2006.02453] [INSPIRE].

[20] G. Tomar, S. Kang and S. Scopel, *Low-mass extension of direct detection bounds on WIMP-quark and WIMP-gluon effective interactions using the Migdal effect*, *Astropart. Phys.* **150** (2023) 102851 [arXiv:2210.00199] [INSPIRE].

[21] W. Wang, K.-Y. Wu, L. Wu and B. Zhu, *Direct detection of spin-dependent sub-GeV dark matter via Migdal effect*, *Nucl. Phys. B* **983** (2022) 115907 [arXiv:2112.06492] [INSPIRE].

[22] K.V. Berghaus, A. Esposito, R. Essig and M. Sholapurkar, *The Migdal effect in semiconductors for dark matter with masses below* $\sim 100\,MeV$, *JHEP* **01** (2023) 023 [arXiv:2210.06490] [INSPIRE].

[23] D. Adams et al., *Measuring the Migdal effect in semiconductors for dark matter detection*, *Phys. Rev. D* **107** (2023) L041303 [arXiv:2210.04917] [INSPIRE].

[24] P. Cox, M.J. Dolan, C. McCabe and H.M. Quiney, *Precise predictions and new insights for atomic ionization from the Migdal effect*, *Phys. Rev. D* **107** (2023) 035032 [arXiv:2208.12222] [INSPIRE].

[25] C. Blanco et al., *Molecular Migdal effect*, *Phys. Rev. D* **106** (2022) 115015 [arXiv:2208.09002] [INSPIRE].

[26] Y.-F. Li and S.-Y. Xia, *Migdal effect of Phonon-mediated neutrino nucleus scattering in semiconductor detectors*, arXiv:2310.05704 [INSPIRE].

[27] N.F. Bell et al., *Exploring light dark matter with the Migdal effect in hydrogen-doped liquid xenon*, *Phys. Rev. D* **109** (2024) L091902 [arXiv:2305.04690] [INSPIRE].

[28] Y. Gu, J. Tang, L. Wu and B. Zhu, *Probing light DM via the Migdal effect with spherical proportional counter*, *Chin. Phys. C* **47** (2023) 125105 [arXiv:2309.09740] [INSPIRE].

[29] M. Atzori Corona et al., *On the impact of the Migdal effect in reactor CEνNS experiments*, *Phys. Lett. B* **852** (2024) 138627 [arXiv:2307.12911] [INSPIRE].

[30] M. Pospelov, *Neutrino Physics with Dark Matter Experiments and the Signature of New Baryonic Neutral Currents*, *Phys. Rev. D* **84** (2011) 085008 [arXiv:1103.3261] [INSPIRE].

JHEP05(2024)288

[31] R. Harnik, J. Kopp and P.A.N. Machado, *Exploring nu Signals in Dark Matter Detectors*, *JCAP* **07** (2012) 026 [arXiv:1202.6073] [INSPIRE].

[32] J. Billard, L.E. Strigari and E. Figueroa-Feliciano, *Solar neutrino physics with low-threshold dark matter detectors*, *Phys. Rev. D* **91** (2015) 095023 [arXiv:1409.0050] [INSPIRE].

[33] J.B. Dent et al., *Probing light mediators at ultralow threshold energies with coherent elastic neutrino-nucleus scattering*, *Phys. Rev. D* **96** (2017) 095007 [arXiv:1612.06350] [INSPIRE].

[34] D.G. Cerdeño et al., *Physics from solar neutrinos in dark matter direct detection experiments*, *JHEP* **09** (2016) 048 [*Erratum ibid.* **09** (2016) 048] [arXiv:1604.01025] [INSPIRE].

[35] B. Dutta, S. Liao, L.E. Strigari and J.W. Walker, *Non-standard interactions of solar neutrinos in dark matter experiments*, *Phys. Lett. B* **773** (2017) 242 [arXiv:1705.00661] [INSPIRE].

[36] D. Aristizabal Sierra, N. Rojas and M.H.G. Tytgat, *Neutrino non-standard interactions and dark matter searches with multi-ton scale detectors*, *JHEP* **03** (2018) 197 [arXiv:1712.09667] [INSPIRE].

[37] C. Bœhm et al., *How high is the neutrino floor?*, *JCAP* **01** (2019) 043 [arXiv:1809.06385] [INSPIRE].

[38] J. Monroe and P. Fisher, *Neutrino Backgrounds to Dark Matter Searches*, *Phys. Rev. D* **76** (2007) 033007 [arXiv:0706.3019] [INSPIRE].

[39] J.D. Vergados and H. Ejiri, *Can Solar Neutrinos be a Serious Background in Direct Dark Matter Searches?*, *Nucl. Phys. B* **804** (2008) 144 [arXiv:0805.2583] [INSPIRE].

[40] A. Gutlein et al., *Solar and atmospheric neutrinos: Background sources for the direct dark matter search*, *Astropart. Phys.* **34** (2010) 90 [arXiv:1003.5530] [INSPIRE].

[41] C.A.J. O'Hare, *New Definition of the Neutrino Floor for Direct Dark Matter Searches*, *Phys. Rev. Lett.* **127** (2021) 251802 [arXiv:2109.03116] [INSPIRE].

[42] J. Billard, L. Strigari and E. Figueroa-Feliciano, *Implication of neutrino backgrounds on the reach of next generation dark matter direct detection experiments*, *Phys. Rev. D* **89** (2014) 023524 [arXiv:1307.5458] [INSPIRE].

[43] E. Vitagliano, I. Tamborra and G. Raffelt, *Grand Unified Neutrino Spectrum at Earth: Sources and Spectral Components*, *Rev. Mod. Phys.* **92** (2020) 45006 [arXiv:1910.11878] [INSPIRE].

[44] XENON collaboration, *Light dark matter search with ionization signals in XENON1t*, *Phys. Rev. Lett.* **123** (2019) 251801 [arXiv:1907.11485] [INSPIRE].

[45] D.Z. Freedman, *Coherent Neutrino Nucleus Scattering as a Probe of the Weak Neutral Current*, *Phys. Rev. D* **9** (1974) 1389 [INSPIRE].

[46] XENON collaboration, *Search for Light Dark Matter Interactions Enhanced by the Migdal Effect or Bremsstrahlung in XENON1T*, *Phys. Rev. Lett.* **123** (2019) 241803 [arXiv:1907.12771] [INSPIRE].

[47] A.M. Green, *Astrophysical uncertainties on direct detection experiments*, *Mod. Phys. Lett. A* **27** (2012) 1230004 [arXiv:1112.0524] [INSPIRE].

[48] A.J. Deason et al., *The local high-velocity tail and the Galactic escape speed*, *Mon. Not. Roy. Astron. Soc.* **485** (2019) 3514 [arXiv:1901.02016] [INSPIRE].

[49] N. Bozorgnia et al., *Simulated Milky Way analogues: implications for dark matter direct searches*, *JCAP* **05** (2016) 024 [arXiv:1601.04707] [INSPIRE].

JHEP05(2024)288

[50] L. Necib et al., *Under the Firelight: Stellar Tracers of the Local Dark Matter Velocity Distribution in the Milky Way*, arXiv:1810.12301 [DOI:10.3847/1538-4357/ab3afc] [INSPIRE].

[51] N.W. Evans, C.A.J. O'Hare and C. McCabe, *Refinement of the standard halo model for dark matter searches in light of the Gaia Sausage*, *Phys. Rev. D* **99** (2019) 023012 [arXiv:1810.11468] [INSPIRE].

[52] G. Besla, A. Peter and N. Garavito-Camargo, *The highest-speed local dark matter particles come from the Large Magellanic Cloud*, *JCAP* **11** (2019) 013 [arXiv:1909.04140] [INSPIRE].

[53] G. Herrera and A. Ibarra, *Direct detection of non-galactic light dark matter*, *Phys. Lett. B* **820** (2021) 136551 [arXiv:2104.04445] [INSPIRE].

[54] LUX collaboration, *Results of a Search for Sub-GeV Dark Matter Using 2013 LUX Data*, *Phys. Rev. Lett.* **122** (2019) 131301 [arXiv:1811.11241] [INSPIRE].

[55] CDEX collaboration, *Constraints on Spin-Independent Nucleus Scattering with sub-GeV Weakly Interacting Massive Particle Dark Matter from the CDEX-1B Experiment at the China Jinping Underground Laboratory*, *Phys. Rev. Lett.* **123** (2019) 161301 [arXiv:1905.00354] [INSPIRE].

[56] EDELWEISS collaboration, *Search for sub-GeV dark matter via the Migdal effect with an EDELWEISS germanium detector with NbSi transition-edge sensors*, *Phys. Rev. D* **106** (2022) 062004 [arXiv:2203.03993] [INSPIRE].

[57] XENON collaboration, *First Dark Matter Search with Nuclear Recoils from the XENONnT Experiment*, *Phys. Rev. Lett.* **131** (2023) 041003 [arXiv:2303.14729] [INSPIRE].

[58] LZ collaboration, *First Dark Matter Search Results from the LUX-ZEPLIN (LZ) Experiment*, *Phys. Rev. Lett.* **131** (2023) 041002 [arXiv:2207.03764] [INSPIRE].

[59] PandaX-II collaboration, *Search for Light Dark Matter-Electron Scatterings in the PandaX-II Experiment*, *Phys. Rev. Lett.* **126** (2021) 211803 [arXiv:2101.07479] [INSPIRE].

[60] XENON collaboration, *Search for New Physics in Electronic Recoil Data from XENONnT*, *Phys. Rev. Lett.* **129** (2022) 161805 [arXiv:2207.11330] [INSPIRE].

[61] J.F. Nieves, *Electromagnetic properties of majorana neutrinos*, *Phys. Rev. D* **26** (1982) 3152 [INSPIRE].

[62] B. Kayser, *Majorana neutrinos and their electromagnetic properties*, *Phys. Rev. D* **26** (1982) 1662 [INSPIRE].

[63] C. Giunti and A. Studenikin, *Neutrino electromagnetic interactions: a window to new physics*, *Rev. Mod. Phys.* **87** (2015) 531 [arXiv:1403.6344] [INSPIRE].

[64] P. Vogel and J. Engel, *Neutrino Electromagnetic Form-Factors*, *Phys. Rev. D* **39** (1989) 3378 [INSPIRE].

[65] M. Atzori Corona et al., *New constraint on neutrino magnetic moment and neutrino millicharge from LUX-ZEPLIN dark matter search results*, *Phys. Rev. D* **107** (2023) 053001 [arXiv:2207.05036] [INSPIRE].

[66] L.G. Cabral-Rosetti, M. Moreno and A. Rosado, *Dirac neutrino anapole moment*, *AIP Conf. Proc.* **623** (2002) 347 [hep-ph/0206083] [INSPIRE].

[67] E. Bertuzzo et al., *Dark Matter and Exotic Neutrino Interactions in Direct Detection Searches*, *JHEP* **04** (2017) 073 [arXiv:1701.07443] [INSPIRE].

[68] Y. Farzan, M. Lindner, W. Rodejohann and X.-J. Xu, *Probing neutrino coupling to a light scalar with coherent neutrino scattering*, *JHEP* **05** (2018) 066 [arXiv:1802.05171] [INSPIRE].

JHEP05(2024)288

[69] O.G. Miranda et al., *Implications of the first detection of coherent elastic neutrino-nucleus scattering (CEvNS) with Liquid Argon*, *JHEP* **05** (2020) 130 [*Erratum ibid.* **01** (2021) 067] [arXiv:2003.12050] [INSPIRE].

[70] D. Aristizabal Sierra, B. Dutta, S. Liao and L.E. Strigari, *Coherent elastic neutrino-nucleus scattering in multi-ton scale dark matter experiments: Classification of vector and scalar interactions new physics signals*, *JHEP* **12** (2019) 124 [arXiv:1910.12437] [INSPIRE].

[71] M. Hoferichter, J. Ruiz de Elvira, B. Kubis and U.-G. Meißner, *High-Precision Determination of the Pion-Nucleon σ Term from Roy-Steiner Equations*, *Phys. Rev. Lett.* **115** (2015) 092301 [arXiv:1506.04142] [INSPIRE].

[72] J. Billard, J. Johnston and B.J. Kavanagh, *Prospects for exploring New Physics in Coherent Elastic Neutrino-Nucleus Scattering*, *JCAP* **11** (2018) 016 [arXiv:1805.01798] [INSPIRE].

[73] R.N. Mohapatra and R.E. Marshak, *Local b-l symmetry of electroweak interactions, majorana neutrinos, and neutron oscillations*, *Phys. Rev. Lett.* **44** (1980) 1316 [*Erratum ibid.* **44** (1980) 1643] [INSPIRE].

[74] A. Davidson, *$B - L$ as the fourth color within an $\mathrm{SU}(2)_L \times \mathrm{U}(1)_R \times \mathrm{U}(1)$ model*, *Phys. Rev. D* **20** (1979) 776 [INSPIRE].

[75] M. Lindner, T. Rink and M. Sen, *Light vector bosons and the weak mixing angle in the light of new reactor-based CEνNS experiments*, arXiv:2401.13025 [INSPIRE].

[76] S.K. Agarwalla, F. Lombardi and T. Takeuchi, *Constraining Non-Standard Interactions of the Neutrino with Borexino*, *JHEP* **12** (2012) 079 [arXiv:1207.3492] [INSPIRE].

[77] S. Bilmis et al., *Constraints on Dark Photon from Neutrino-Electron Scattering Experiments*, *Phys. Rev. D* **92** (2015) 033009 [arXiv:1502.07763] [INSPIRE].

[78] A.N. Khan, W. Rodejohann and X.-J. Xu, *Borexino and general neutrino interactions*, *Phys. Rev. D* **101** (2020) 055047 [arXiv:1906.12102] [INSPIRE].

[79] P. Coloma et al., *Constraining new physics with Borexino Phase-II spectral data*, *JHEP* **07** (2022) 138 [*Erratum ibid.* **11** (2022) 138] [arXiv:2204.03011] [INSPIRE].

[80] Y.-F. Li and S.-Y. Xia, *Constraining light mediators via detection of coherent elastic solar neutrino nucleus scattering*, *Nucl. Phys. B* **977** (2022) 115737 [arXiv:2201.05015] [INSPIRE].

[81] M. Demirci and M.F. Mustamin, *Solar neutrino constraints on light mediators through coherent elastic neutrino-nucleus scattering*, *Phys. Rev. D* **109** (2024) 015021 [arXiv:2312.17502] [INSPIRE].

[82] T. Schwemberger, V. Takhistov and T.-T. Yu, *Hunting Nonstandard Neutrino Interactions and Leptoquarks in Dark Matter Experiments*, arXiv:2307.15736 [INSPIRE].

[83] V. De Romeri, D.K. Papoulias and C.A. Ternes, *Light vector mediators at direct detection experiments*, arXiv:2402.05506 [INSPIRE].

[84] D.W.P. Amaral, D. Cerdeño, A. Cheek and P. Foldenauer, *A direct detection view of the neutrino NSI landscape*, *JHEP* **07** (2023) 071 [arXiv:2302.12846] [INSPIRE].

[85] R. Essig et al., *Snowmass2021 Cosmic Frontier: The landscape of low-threshold dark matter direct detection in the next decade*, in the proceedings of the *Snowmass 2021*, Seattle, U.S.A., July 17–26 (2022) [arXiv:2203.08297] [INSPIRE].

JHEP05(2024)288